Journal of Alloys and Compounds 513 (2012) 318–323

Contents lists available at SciVerse ScienceDirect

Journal of Alloys and Compounds

journal homepage: www.elsevier.com/locate/jallcom

Enhanced stokes shift of $S_2 \rightarrow S_0$ emission and structural investigations of Sn(IV)Porphyrins doped hybrid borate glasses

N. Venkatramaiah[a], Buthanapalli Ramakrishna[a], A. Raveendra Kumar[a], N. Veeraiah[b], R. Venkatesan[a,*]

[a] Department of Chemistry, School of Physical Chemical and Applied sciences, Pondicherry University, Puducherry 605014, India
[b] Department of Physics, Acharya Nagarjuna University, Nuzvid Campus, Nuzvid 521 201, A.P., India

ARTICLE INFO

Article history:
Received 19 July 2011
Received in revised form
15 September 2011
Accepted 15 September 2011
Available online 25 October 2011

Keywords:
Hybrid borate glass
Sn(IV)Porphyrins
Optical properties
Micro-Raman
Luminescence

ABSTRACT

In the present study, we report our results on Sn(IV)TPP and its derivatives doped hybrid borate glasses. The photophysical and structure of Sn(IV)Porphyrins in borate glass matrix was studied through micro-Raman, optical absorption, steady state and time resolved fluorescence emission techniques. The optical absorption spectrum shows red shift in Soret band and change in the intensity of Q-bands. Upon exposure to UV light at 260 nm, the glass samples exhibit strong blue emission and red emission at 365 nm. Steady state fluorescence emission spectrum of hybrid glasses exhibits dual emission bands originating from the $S_2 \rightarrow S_0$ and $S_1 \rightarrow S_0$ states. The appearance of large stokes shift ($\Delta\upsilon$), enhanced $S_2 \rightarrow S_0$ emission at ~482 nm and excitation dependent of $S_1 \rightarrow S_0$ emission indicates that the structure of Sn(IV)Porphyrins were inherently modified in the borate glass matrix. Time resolved fluorescence of $S_2 \rightarrow S_0$ emission was found to be in the range of 0.23–0.36 ns, $S_1 \rightarrow S_0$ emission shows 1.23–1.57 ns and 9.12–9.63 ns, respectively. The results obtained in glass matrix were correlated with solution medium and the possible structures were investigated.

1. Introduction

Porphyrins are the versatile organic chromophores for the design of novel artificial photosynthetic supra molecular systems [1]. In particular, Sn(IV)Porphyrins have been of great interest because of its metal–ligand interactions could provide a convenient method for construction of functional supra-molecular building blocks [2]. The physicochemical properties of these compounds are very sensitive to modifications of the electronic distribution on the aromatic ring. Thus, they serve as probes to study the environment in which they reside [3]. Study on electron transfer from the higher excited state to first excited state is rather limited, because of the quite short lifetimes of these intermediates [4]. However, trapping of organic dyes in solid rigid matrix decreases the rate of electron transfer occurs from the higher excited state to the lowest excited state provides the mechanism for excited state charge transfer process in various photo induced processes. Immobilization of Sn(IV)Porphyrins in sol–gel and polymer matrices has previously been reported in the literature [5,6]. It's biological importance as photosensitizer has prompted to study the photophysics of Sn(IV)Porphyrins in different environments [3]. The photophysical properties of these compounds in polymer and thin film matrices were found to be different from that of solution medium [7].

Encapsulation of dyes in glass matrix gives new photosensitive materials with a great variety of possible compositions [8]. Langford et al. have introduced bis(silyloxy)tin(IV) porphyrins into silica beads for producing novel photochromic glasses the prospective applications as organic solar cells [9]. Delmarre et al. have reported the environment effect of on the photophysical behaviour of Sn(IV)Porphyrinon zirconium–silica hybrid network [10]. Trapping of different freebase porphyrins into borate glass matrix shows promising materials for the prospective applications as optical materials and tunable band pass filters [11,12]. Wen et al. have reported the non-linear optical (NLO) properties of Sn(IV)Porphyrin doped borate glasses. These hybrid materials exhibit large third order non-linear susceptibility (χ^3) and behave as good optical limiting materials [13]. However, the detailed investigations on the structure and photophysical properties of Sn(IV)Porphyrins in borate glass network was not explored. Understanding the structure and property relationship would help to researchers to design new functional materials for the prospective applications. The interaction between borate network and organic molecules leads to the enhanced gradients of the ground state dipole moments leading to interesting changes in spectroscopic properties [8]. Hence, in the present paper we have modeled a series of Sn(IV)Porphyrins doped hybrid borate glasses to investigate the photophysical properties (viz., optical absorption, micro-Raman, steady state and time

---

[*] Corresponding author. Tel.: +91 413 2654415; fax: +91 413 2656 740.
E-mail address: venkatesan63@yahoo.com (R. Venkatesan).

0925-8388/$ – see front matter © 2011 Elsevier B.V. All rights reserved.
doi:10.1016/j.jallcom.2011.09.105

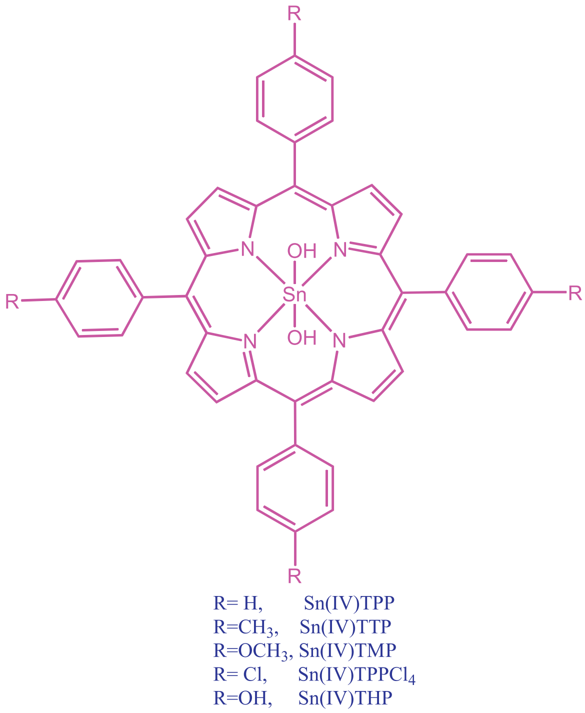

Fig. 1. Molecular structure of Sn(IV)Porphyrins.

resolved fluorescence) to understand more insight into the structure of Sn(IV)Porphyrins in borate glass matrix. The results obtained in glass were correlated with those in solution medium and possible structures of Sn(IV)Porphyrins in borate glass was studied.

2. Materials and methods

A series of freebase porphyrins and its Sn(IV)Porphyrins were synthesized according to known procedure described earlier [14]. Sn(IV)Porphyrins doped hybrid borate glasses were prepared by rapid melt quench technique [15]. In brief, weighed quantities of boric acid (12 g) and 2 mg of various Sn(IV)Porphyrins (Fig. 1) were thoroughly mixed in an agate mortar and melted in porcelain crucible at 150 °C in a muffle furnace for 5 h. The temperature was rapidly raised to 230 °C for 30 min to obtain bubble free melt. The melt was poured on preheated brass mould to obtain the circular glass discs of 2 mm thickness and 1 cm diameter. To obtain the optical quality, the glass samples were polished with water free lubricants such as diamond paste (3 μm size) and were stored over CaCl$_2$. Differential scanning calorimetric analysis (DSC) of these samples was carried out by TA instruments Model Q20 V24.2 Build 107 with heating rate of 5 °C min^{-1} in the temperature range 30–500 °C. The amorphous nature of the samples was studied by using PANanalytical X′-pert PRO X-ray diffractometer with Cu Kα radiation. Raman spectra of the hybrid glasses was acquired using a confocal micro-Raman probe instrument in which Raman scattering was excited with 488 nm radiation from a Spex 2000 argon ion laser. Raman scattering was collected in a backscattering configuration using microscope objective and directed through a THR-1000 (JY) spectrograph, equipped with a 1200 groove/mm grating and a holographic notch filter, to a Spex-View 2D CCD detector controlled by Spectromax software. Optical absorption spectrum was recorded on Ocean optics (HR4000) spectrophotometer. Steady-state fluorescence and phosphorescence emission studies were carried out with a Spex FluoroLog-3 spectrofluorometer (Jobin-Yvon Inc.) with pulsed Xenon lamp (450 W). Time resolved fluorescence measurements were performed using the time-correlated single-photon counting (TCSPC) with pico second LED (459 nm; FWHM <200 ps) with repetition rate of 1 MHz was used to excite the samples. The photons collected at the detector are correlated by a time-to-amplitude converter (TAC) to the excitation pulse. Signals were collected using an IBH data station Hub photon counting module and data analysis was performed using the commercially available DAS6 software (HORIBA JobinYvon IBH).

3. Results and discussion

The hybrid glass samples prepared were free from visible inhomogeneities, such as inclusions, cracks or bubbles. Based upon the visual examination, the absence of peaks in the X-ray diffraction pattern and absence of crystalline phases in SEM pictures, we could come to the conclusion that the samples prepared were of amorphous nature [11]. From the measured values of density (ρ), other physical parameters such as average molecular weight, refractive index (n), molecular ion concentration (N_i), intermolecular separation (R_i) were calculated and are presented in Table 1. The density of Sn(IV)Porphyrin doped borate glasses were found to be in the range 1.91–2.08 g/cm^3 indicate that borate network consisting of mainly –BO$_3$ units [16]. The variation in the density is due to variation in the structural motifs introduced into the glass matrix. All the hybrid glass samples show glass transition temperature (T_g) at ~109 ± 1 °C and decomposition of Sn(IV)Porphyrins observed at 423 °C [17].

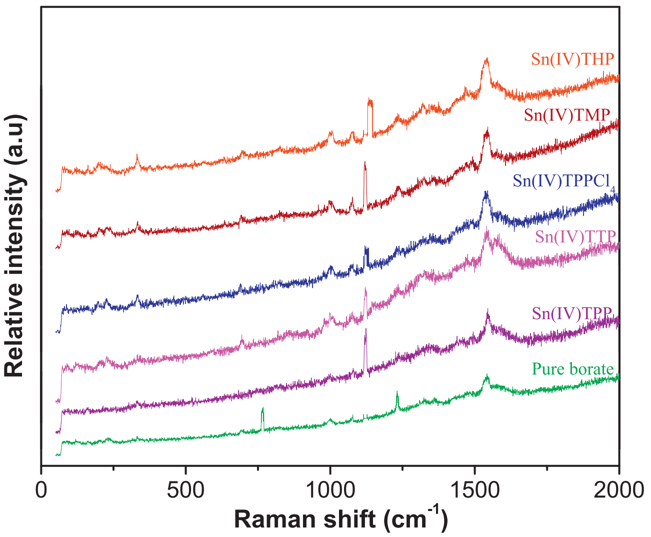

Fig. 2. Micro-Raman spectra of various Sn(IV)Porphyrins doped borate glasses.

The micro-Raman spectra of Sn(IV)Porphyrins doped borate glasses is shown in Fig. 2. The micro-Raman spectrum of vitreous B$_2$O$_3$ shows a peak at ~776 cm^{-1} corresponds to the boroxol ring and the band at 1231 cm^{-1} corresponds to pyroborate units originate from the symmetric stretching vibration of B–O–B bridges and terminal B–O bonds of borate network. The appearance of the peak 1544 cm^{-1} arises due to BΦ_2O$^-$ triangles (Φ = bridging oxygen) linked to BΦ^{4-} units and BΦ_2O$^-$ triangles linked to other BO$_3$ units [18]. The appearance of new peaks at 220, 390, 1190, 1270, 1420

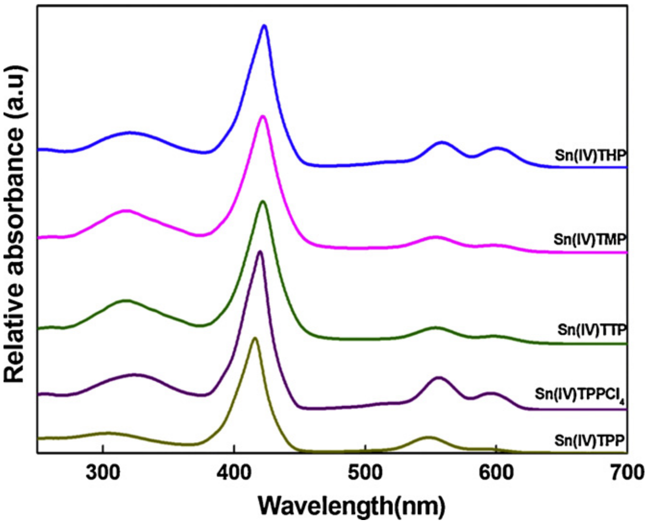

Fig. 3. Optical absorption spectra of various Sn(IV)Porphyrins doped borate glasses.

Table 1
The physical and optical data of various Sn(IV)Porphyrins doped borate glasses.

Porphyrin	Density (g/cm^3)	Refractive index (n)	Molecular ion conc. (N_i) (1×10^{18} mol/cm^3)	Inter molecular separation, R_i (nm)	E_g (eV)	E_u (eV)	T_g (°C)
Sn(IV)TPP	1.912	2.12	1.814	8.112	3.21	0.321	108
Sn(IV)TTP	1.925	2.26	1.703	8.457	2.95	0.338	109
Sn(IV)TMP	1.997	2.19	1.597	8.678	2.77	0.361	109
Sn(IV)TPPCl$_4$	2.014	2.18	1.612	8.713	2.87	0.348	108
Sn(IV)THP	2.087	2.32	1.678	8.532	2.54	0.393	111

and 1490 cm^{-1} in Sn(IV)Porphyrin doped glasses are corresponds to the porphyrin skeleton [19]. The appearance of major intense peak at 1270 cm^{-1} corresponds to phenyl vibrations. The shift in the peak vibrations from 1002 cm^{-1} (pure borate) to 1030 cm^{-1} in Sn(IV)Porphyrin doped glasses indicate that Sn(IV)Porphyrins undergone strong interaction with borate network.

3.1. *Optical absorption*

The optical absorption spectra of various Sn(IV)Porphyrins doped hybrid borate glasses are shown in Fig. 3. The absorption spectrum shows a strong near-UV Soret (B) band (corresponding to $S_0 \rightarrow S_2$) at ~420 nm and a pair of weaker visible Q(1,0) and Q(0,0) bands (corresponding to $S_0 \rightarrow S_1$) appears at ~550 nm and ~600 nm, respectively. The peak at ~313 nm arises due to the $n \rightarrow \pi^*$ transitions. The full width half maxima (FWHM) of the Soret band increases in the order of Sn(IV)TPP < Sn(IV)TTP < Sn(IV)TMP < Sn(IV)TPPCl$_4$ and <Sn(IV)THP. However, Sn(IV)THP shows ~11 nm red shift in Soret band and ~18 nm red shift in the Q-band over Sn(IV)TPP doped glass. This can be attributed due to increase in the electron donating groups on the phenyl ring will increase the electron donating tendency and rising of the electron density on the a_{2u} orbital and significant stabilization of the lowest unoccupied molecular orbital (LUMO) energy level with a decrease in the symmetry of the porphyrin skeleton [20]. It is also found that the intensity ratio Q(1,0) to Q(0,0) bands is higher for Sn(IV)TPPCl$_4$ and Sn(IV)THP doped glasses. The change in the Q(0,0)/Q(1,0) intensity ratio with different substituents reflects changes in the relative energies of the frontier molecular orbitals and thus the overall oscillator strength of the $S_0 \rightarrow S_1$ absorption contour [5].

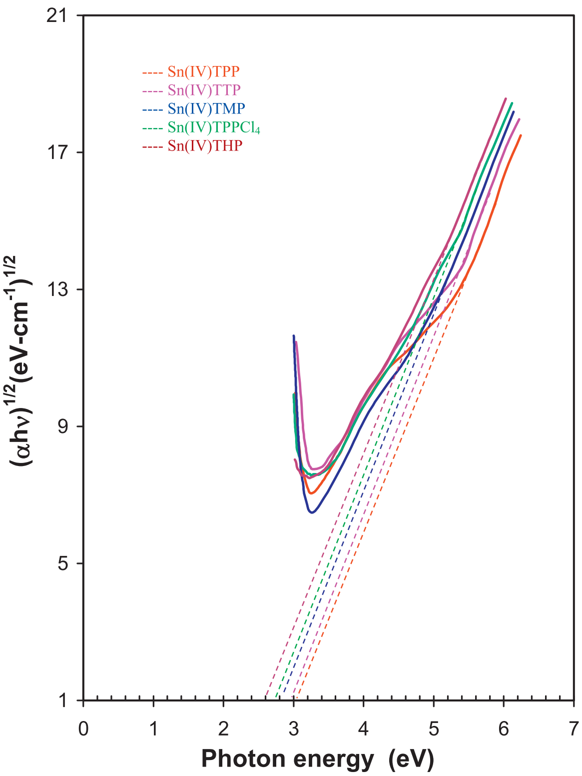

Fig. 4. Optical band gap pattern of various Sn(IV)Porphyrins doped borate glasses.

On compare the results obtained in glass to the solution medium, glass samples exhibits red shift of 3–10 nm and more broaden in the Soret band. Since axial ligation to a metalloporphyrins result in red shift of all the absorption features and a change in the intensity of the Q(1,0) band with respect to the Q(0,0) band. This reveals that Sn(IV)Porphyrins forms axial coordination with –BO$_3$ units of the glass network. The optical band gap (Fig. 4) and urbach's energy was calculated as described earlier [15] and the pertinent data is summarized in Table 1. The E_g values were found to vary with the nature of substituents on the phenyl ring of Sn(IV)Porphryin and are closely related to the energy band gap between valance band and conduction band. The average E_u values ~0.36 ± 0.03 eV suggests that bonding in these materials is similar to borate glasses obtained at high temperatures [21].

3.2. *Steady state emission*

Fig. 5 shows steady state fluorescence emission spectra of various Sn(IV)Porphyrins doped borate glasses. On excitation at 420 nm, all Sn(IV)Porphyrins exhibits two emission bands in the range 600–668 nm corresponding to $S_1 \rightarrow S_0$ transition and another strong emission at ~482 nm corresponding to $S_2 \rightarrow S_0$ transition. The emission data for all Sn(IV)Porphyrins in borate glass was summarized in Table 2. The shape of $S_1 \rightarrow S_0$ emission is broadened and a significant red shift in the glass matrix is observed as compared with the counterpart in solution. The red shift of 20–30 nm and broadening in $S_1 \rightarrow S_0$ emission in glass matrix arises due to formation of complex with borate network and difference in the environment. On the other hand, a broad $S_2 \rightarrow S_0$ emission is observed at ~482 nm with FWHM of ~50 nm. The

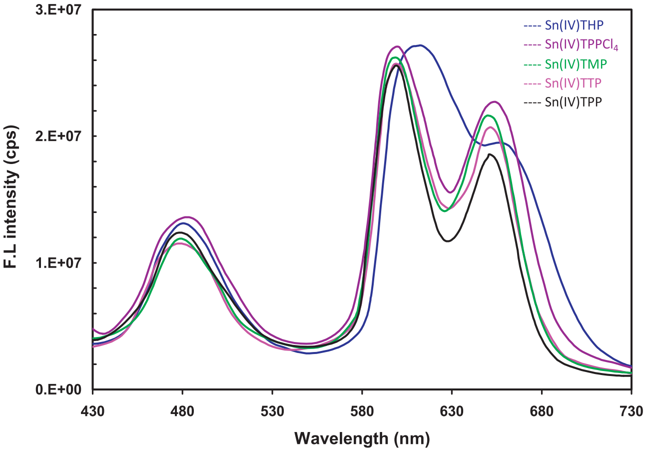

Fig. 5. Steady state fluorescence emission spectra of various Sn(IV)Porphyrins doped glasses on excitation at 420 nm.

Table 2
Optical absorption, emission and fluorescence lifetime data of various Sn(IV)Porphyrins doped borate glasses. The values in the parenthesis indicate relative amplitudes of fluorescent species.

Porphyrin	Optical absorption		Fluorescence emission		Stokes shift	Fluorescence lifetime in ns (λ_{em} = 482 nm)			
	S (nm)	Q (nm)	λ_{ex} (nm)	λ_{em} (nm)	$\Delta\upsilon$ (nm)	τ_1 (A_1%)	τ_2 (A_2%)	τ_3 (A_3%)	χ^2
Sn(IV)TPP	416	549, 591	420	478, 605, 661	62	0.21 (35.2)	1.42 (45.63)	9.16 (19.17)	1.023
Sn(IV)TTP	422	555, 603	420	486, 607, 663	64	0.23(40.21)	1.43(42.17)	9.21 (19.17)	1.016
Sn(IV)TMP	424	556, 606	420	490, 608, 668	66	0.31 (41.16)	1.57 (40.17)	9.03 (18.67)	1.064
Sn(IV)TPPCl$_4$	420	555, 597	420	485, 602, 666	65	0.27 (46.12)	1.17 (41.32)	8.06 (12.56)	1.087
Sn(IV)THP	427	558, 609	420	493, 610, 671	67	0.36 (51.89)	1.16 (38.16)	9.14 (9.94)	1.054

Precision is ±0.06 ns.

Table 3
Optical absorption, emission and fluorescence lifetime decay data of various Sn(IV)Porphyrins in dichloromethane medium.

Porphyrin	Absorption data		Fluorescence emission	Fluorescence lifetime (λ_{em} = 590 nm)	
	S (nm)	Q (nm)	λ_{max} (nm)	τ (ns)	χ^2
Sn(IV)TPP	413	547, 589	430, 591, 631	0.82	1.056
Sn(IV)TTP	415	555, 592	431, 591, 632	0.86	1.089
Sn(IV)TMP	420	559, 601	434, 597, 640	0.91	1.093
Sn(IV)TPPCl$_4$	415	555, 590	430, 593, 634	0.80	1.067
Sn(IV)THP	421	561, 597	438, 605, 655	0.89	1.081

Precision is ±0.06 ns.

intensity of $S_2 \rightarrow S_0$ emission is found to be nearly half to that of $S_1 \rightarrow S_0$ emission. The $S_2 \rightarrow S_0$ emission exhibit large stokes shift of ~52 nm and is more sensitive to the nature of the substituents. In contrast, Sn(IV)Porphyrins shows very weak $S_2 \rightarrow S_0$ emission at ~430 nm in solution medium and at low temperatures with stokes shift of 5–10 nm [22,23]. The pertinent data on optical, emission and lifetime data of various Sn(IV)Porphyrins in dichloromethane is summarized in Table 3. Interesting features were observed by change in the excitation wavelength. For Sn(IV)THP doped glass (Fig. 6a), the position of $Q(0,0)$ emission band was found to be varied with excitation wavelength and show displacement up to 25 nm. The fluorescence excitation spectrum for $Q(0,0)$ band emission confirms that emission actually arises from the excited electronic states of Soret band. The excitation wavelength was found to varied dependent on the emission wavelength (Fig. 6b). This further confirms that in borate glass Sn(IV)THP exists in different structures. The emission wavelength of $Q(0,0)$ band increases linearly with increase in the excitation wavelength. This strongly reflects on the various photo induced nonlinear optical properties. Since borate glasses possess very rare possibility to change the degree of crystallanity. Second-order non-linear optical effects in BiB_3O_6 glass fibers which may be principal change to the observed processes of photo-induced optical transfer. The same features also influence on the nonlinear optical susceptibilities [24,25].

Fig. 7 shows the phosphorescence emission spectra of Sn(IV)Porphyrins doped hybrid glasses. The spectra exhibits two emission peaks at ~782 nm and ~882 nm corresponding to $T(0,0)$ and $T(0,1)$ respectively. The intensity ratio of $T(0,1)/T(0,0)$ is found to 0.28. This arises due to strongly allowed and quasi forbidden of the triplet states, i.e. in porphyrin the lowest triplet state is largely either $^3(a_{1u}(\pi) \rightarrow \text{e.g.}(\pi^*)$ and $^3(a_{2u}(\pi) \rightarrow \text{e.g.}(\pi^*)$. Both these states have direct spin orbit coupling to the Soret band. Hence, $T(0,0)$ band is relatively intense compared to the $T(0,1)$. A similar results were also observed for other Sn(IV)Porphyrins doped glasses. Fig. 8 shows the photograph of various Sn(IV)Porphyrins doped hybrid glasses exposed to UV light at 260 nm and 365 nm. Upon exposed to 260 nm, the hybrid glasses show intense blue emission and red emission observed at 365 nm which corresponds to the $S_2 \rightarrow S_0$ and $S_1 \rightarrow S_0$ emission. The large enhancement in $S_2 \rightarrow S_0$ emission implying that distortion in the Sn(IV)Porphyrin symmetry leads to slower in the radiative electron transfer from S_2 to S_1. This results in appearance of strong blue $S_2 \rightarrow S_0$ emission of Sn(IV)Porphyrins in borate glass.

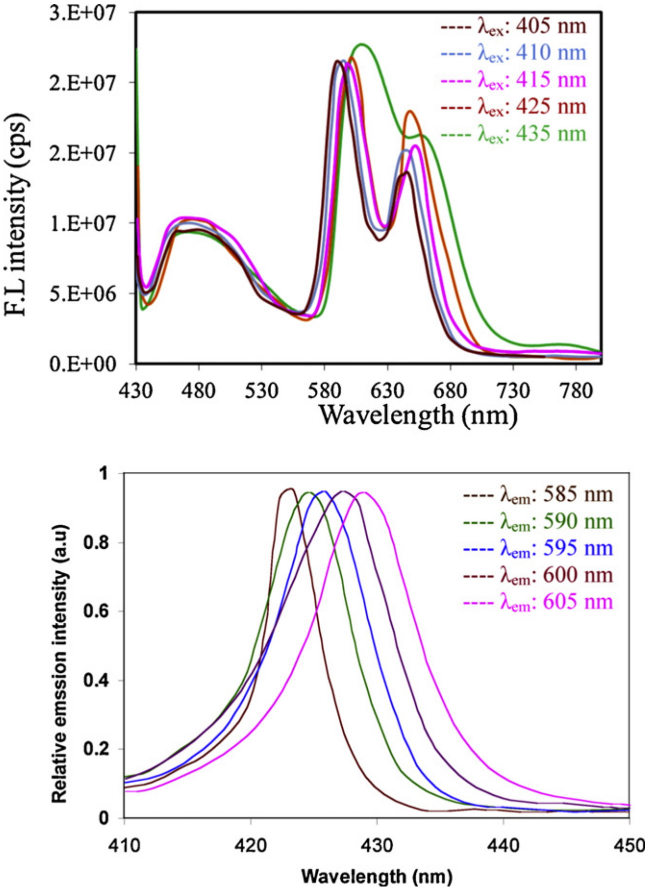

Fig. 6. (a) Fluorescence emission spectra of Sn(IV)THP doped borate glass at different excitation wavelengths, (b) fluorescence excitation spectra of Sn(IV)THP doped borate glass at different emission wavelengths.

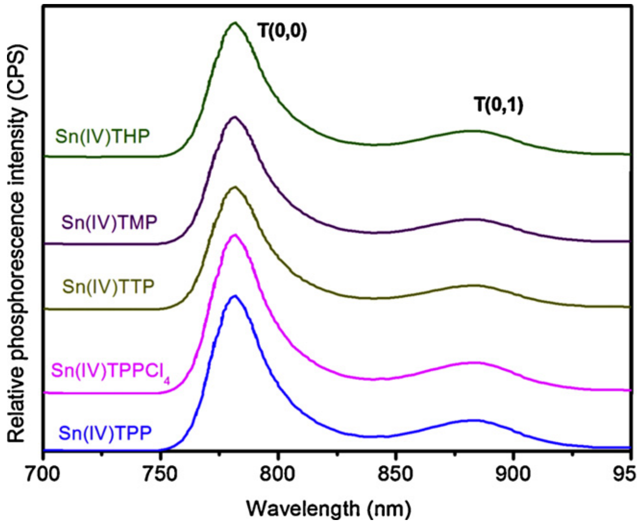

Fig. 7. Phosphorescence emission spectra of various Sn(IV)Porphyrins doped glasses.

3.3. Time resolved fluorescence emission

To explore the deactivation processes in detail, the $S_1 \rightarrow S_0$ and $S_2 \rightarrow S_0$ fluorescence lifetimes of Sn(IV)Porphyrin doped glasses were measured by TCSPC technique and the decay profiles are shown in Fig. 9. For all Sn(IV)Porphyrins, the $S_1 \rightarrow S_0$ fluorescence lifetime (Fig. 9b) with 459 nm LED (FWHM < 200 ps) shows two exponential decay with lifetime in the range $\tau_1 = 1.23–1.57$ ns and $\tau_2 = 9.12–9.63$ ns with relative amplitudes of 64–68% and 32–36%, respectively. This indicates that two structurally modified porphyrins were exists in the glass matrix. This is completely in contrast to the observation of single exponential decay with lifetime of ~0.86 ns [26]. The appearance of long lifetime (τ_2) was similar to those observed in the freebase porphyrins [11]. Since boric acid behaves as a strong acid in molten state, a part of Sn atom gets demetallated from the central core of the porphyrin and behaves like freebase porphyrin. The second lifetime (τ_1) with major amplitude corresponding to the complexed form of Sn(IV)Porphyrins with two $-BO_3$ units axially and forms as a trimer similar to Sn(IV)Porphyrin trimer scaffolds [27]. The decrease in the short lifetime (τ_1) for Sn(IV)THP and Sn(IV)$TPPCl_4$ indicates that in addition to axial coordination peripheral coordination also occurs in these molecules. On the other hand, the $S_2 \rightarrow S_0$ emission at 482 nm exhibits three lifetimes 0.23–0.36 ns, 1.18–1.52 ns and 9.12–9.63 ns respectively (Fig. 9a). On compare both $S_1 \rightarrow S_0$ and $S_2 \rightarrow S_0$ state lifetimes, it is clear to understand that the lifetimes in the range 0.23–0.36 ns correspond to the $S_2 \rightarrow S_0$ emission. However, the $S_2 \rightarrow S_0$ lifetime of Sn(IV)Porphyrins were found to be ~1–2 ps in solution [22]. This clearly suggests that in borate glass matrix, the excited electronic states of Sn(IV)Porphyrins are trapped that reflects in large enhancement in the lifetimes.

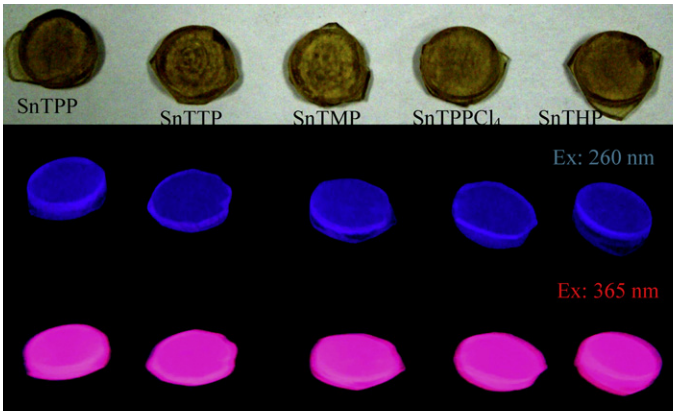

Fig. 8. (a) Photograph of various Sn(IV)Porphyrins doped glasses, (b) hybrid glasses exposed at 260 nm light and (c) hybrid glasses exposed at 365 nm light.

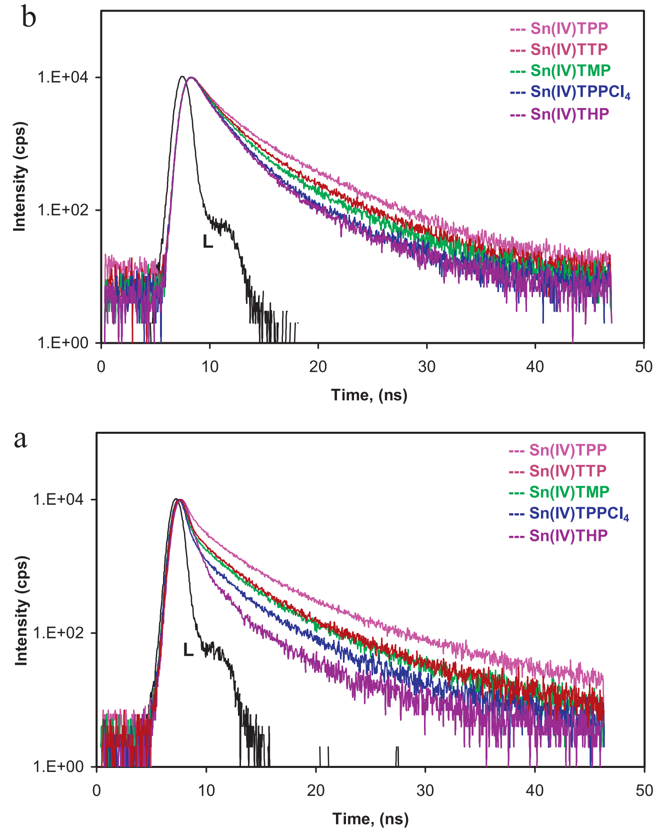

Fig. 9. Time resolved fluorescence spectra of various Sn(IV)Porphyrins doped borate glasses (a) for emission at $\lambda_{em} = 482$ nm (b) for emission at $\lambda_{em} = 605$ nm. The curve *L* represents the instrument response function.

4. Conclusion

In summary, a series of Sn(IV)Porphyrins were successfully incorporated into borate glass matrix. The optical and photophysical investigation clearly demonstrates the existence of different porphyrins structures in the glass matrix. The variations in the emission spectra with the excitation wavelength indicates grafting of different structures of Sn(IV)Porphyrins in the glass network. This clearly reflects in large enhancement of third order nonlinear susceptibilities. Trapping different excited electronic states in borate glass matrix leads enhancement in the emission and lifetime properties. Attempts were made to incorporate various other metallo porphyrins (M = Zn Cu, Ni, Co, Pt, Pd, etc.) into borate glass matrix. However, in most of the cases demetallation occurs during the hybrid glass formation and behaves like a freebase porphyrin doped hybrid glasses.

Acknowledgements

The authors NVR and RV are thankful to the Council of Scientific and Industrial Research (CSIR), Govt. of. India, New Delhi, for funding the research project (01(2087)/06/EMR-II). The authors are also grateful to Central Instrumentation Facility (CIF), Pondicherry University for instrumentation facility. We also thank to Prof.

D. Narayana Rao, School of Physics, University of Hyderabad for extending the micro-Raman facility.

References

[1] P. Prashanth kumar, B.G. Maiya, Proc. Indian Natl. Sci. Acad. 69 (2003) 83.
[2] D.P. Arnold, J. Blok, Coord. Chem. Rev. 248 (2004) 299.
[3] E.J. Land, A.F. Mcdonaght, D.J. Mcgarvery, T. George Truscott, Proc. Natl. Acad. Sci. 85 (1988) 5429.
[4] V. Ramamurthy, K.S. Schanze (Eds.), Molecular and Supramolecular Photochemistry, Marcel Dekker, New York, 2000, p. 215.
[5] Y. Chen, B. Zhang, J.G. Chen, D.Y. Huang, Spec. Chim. Acta Part A 57 (2001) 2451.
[6] J.A. O'Brien, S. Rallabandi, U. Tripathy, M.F. Paige, R.P. Steer, Chem. Phys. Lett. 475 (2009) 220.
[7] M. Duan, J. Li, G. Mele, C. Wang, X. Fei Lu, G. Vasapollo, F. Xing Zhang, J. Phys. Chem. C 114 (2010) 7857.
[8] H.M. Buck, W.Th.A.M. Vanderlugt, L.J. Oosterhoff, Tetrahedron 19 (1963) 173.
[9] S.J. Langford, M.J. Latter, J. Beckmann, Inorg. Chem. Commun. 8 (2005) 920.
[10] D. Delmarre, A.V.V. Lemarinier, C. Bied Charreton, J. Lumin. 82 (1999) 57.
[11] N. Venkatramaiah, R. Venkatesan, Mater. Chem. Phys. 125 (2011) 729.
[12] N. Venkatramaiah, V.C. Soorya, R. Venkatesan, Physica B 406 (2011) 556.
[13] T.C. Wen, L.C. Hwang, W.Y. Lin, C.H. Chen, C.H. Wu, Chem. Phys. 286 (2003) 293.
[14] K.M. Kadish, D. Dubois, S. Koeller, J.M. Barbe, R. Guilard, Inorg. Chem. 31 (1992) 3292.
[15] N. Venkatramaiah, N. Veeraiah, R. Venkatesan, J. Alloys Compd. 509 (2011) 2797.
[16] W.A. Pisarski, J. Pisarska, W.R. Romanowski, J. Mol. Struct. 744–747 (2005) 515.
[17] N. Venkatramaiah, R. Venkatesan, Solid State Sci. 13 (2011) 616.
[18] E.I. Kamitsos, G.D. Chryssikos, J. Mol. Struct. 247 (1991) 1.
[19] C. Guo, Bin Ren, D.L. Akins, J. Phys. Chem. B 102 (1998) 8751.
[20] M. Meot-Ner, A.D. Adler, J. Am. Chem. Soc. 97 (1975) 5107.
[21] J.D. Dow, D. Redfield, Phys. Rev. B 5 (1972) 594.
[22] M. Maiti, B.R. Danger, R.P. Steer, J. Phys. Chem. A 113 (2009) 11318.
[23] J.M. Vanderkooi, F. Adar, M. Erecinska, Eur. J. Biochem. 64 (1976) 381.
[24] I.V. Kityk, W. Imiolek, A. Majchrowski, E. Michalski, Opt. Commun. 219 (2003) 421.
[25] I.V. Kityk, A. Majchrowski, Opt. Mater. 25 (2004) 33.
[26] P. Prem Kiran, D. Raghunath Reddy, B.G. Maiya, A.K. Dharmadhikari, G. Ravindra Kumar, D. Narayana Rao, Opt. Commun. 252 (2005) 150.
[27] A. Ashok Kumar, L. Giribabu, D. Raghunath Reddy, B.G. Maiya, Inorg. Chem. 26 (2001) 6757.